Effect of asymmetric cooling of sessile droplets on orientation of the freezing tip
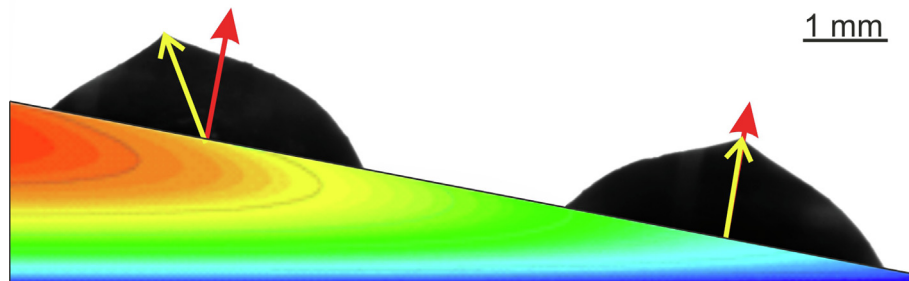
Anton Starostin [a], Vladimir Strelnikov [a], Leonid A. Dombrovsky [b,c,d], Shraga Shoval [e], Oleg Gendelman [f,*], Edward Bormashenko [b,*]

[a] Institute of Technical Chemistry, Academician Korolev St, 3, Perm 614013, Russia
[b] Chemical Engineering Department, Faculty of Engineering, Ariel University, P.O.B. 3, 407000 Ariel, Israel
[c] X-BIO Institute, University of Tyumen, 6 Volodarskogo St, Tyumen 625003, Russia
[d] Heat Transfer Department, Joint Institute for High Temperatures, 17A Krasnokazarmennaya St, Moscow 111116, Russia
[e] Department of Industrial Engineering and Management, Faculty of Engineering, Ariel University, P.O.B. 3, 407000 Ariel, Israel
[f] Faculty of Mechanical Engineering, Technion−Israel Institute of Technology, Haifa 3200003, Israel

G R A P H I C A L A B S T R A C T

A R T I C L E I N F O

A B S T R A C T

Hypothesis: The shape of the "freezing tip" formed by the crystallization of water droplets demonstrated remarkable universality - no dependence on the cooling rate and physico-chemical properties of the substrate has been observed. At the same time, the spatial orientation of the freezing cone may be varied. We hypothesized that the orientation of the freezing tip is determined by the direction of heat flux at the base of the sessile droplet. This direction is expected to be changed when the substrate with a low thermal diffusivity is not cooled uniformly.

Experiments: We studied the freezing of water droplets placed on the inclined surface of wedges made from a variety of materials (polymers: Polymethylmethacrylate, Polytetrafluoroethylene, Polyurethane and metal: Titanium), which were cooled from below. The shape of the frozen droplets was controlled *in situ*.

Computations: The computational model was suggested for the transient temperature field in the polymer wedge to determine a time variation of the local heat flux under the droplets. A comparison of numerical results and the measurements enabled us to confirm the aforementioned hypothesis relating the orientation of the freezing tips to the direction of the heat flux.

* Corresponding authors.
  E-mail addresses: ovgend@technion.ac.il (O. Gendelman), edward@ariel.ac.il (E. Bormashenko).

Findings: It was established that the orientation of the freezing cone axis depends on the location of the frozen droplet on the inclined surface of the wedge. Calculations of the transient temperature field of the wedge confirmed our hypothesis about the physical reason of the various spatial orientations of the freezing cones.

1. Introduction

The study of icing problems is rather important and most challenging from both a fundamental and an engineering point of view [1–8]. Ice formation plays an important role in the operation of power lines, aircrafts, wind turbines and solar panels [1–6]. The freezing of a water droplet on a solid surface is a complex, multistep process involving various thermo-physical and interfacial phenomena [9–14] including heat transfer [10], phase transitions [10], behavior of dissolved gases [13,14], and contact angle hysteresis [11]. In particular, it was found that the time scale inherent for the delay in ice formation has a clear correlation with contact angle hysteresis [11].

At the final stage of freezing, the formation of the so-called "freezing tip" was observed in numerous studies [15–21]. The formation of the freezing tip singularity is a fascinating counterintuitive phenomenon. Sharp, pointy singularities occur rarely due to their high energy concentration. The freezing tip shape demonstrates surprising insensitivity to the freezing conditions [15–20]. The opening angle of the freezing tip is not sensitive to the volume of the droplet, temperature of the substrate and velocity of cooling [15–18]. It has been recently demonstrated that the frozen droplets containing nanosuspensions exhibit a flat plateau shape (instead of a "freezing tip") and such a plateau gets larger with increasing particle concentrations [21]. Transition from the freezing tip to plateau shape was also observed for nanofluid droplets placed on the superhydrophobic surfaces [22].

It was also shown that the shape of a freezing water droplet can be sensitive to the presence of impurities [20]. In addition, it has been demonstrated that the formation of a freezing tip is inherent not only for water droplets but also for the so-called liquid marbles, namely droplets coated with colloidal particles [23,24]. The mechanism of formation of the freezing tip remains largely mysterious. In our recent study, we addressed the freezing of water droplets in different configurations, including "upward" droplets, droplets placed on an inclined plane and droplets placed on greased surfaces [25]. Our research strengthens the idea that the shape of the freezing tip is of a universal nature, only slightly depends on the freezing rate, gravity, the velocity of evaporation, the interfacial properties and spatial orientation of the supporting substrates, and on the surface tension of the frozen liquid [25]. The present study demonstrates that the orientation of the freezing tip follows the temperature gradient (or heat flux direction) in the cooled water droplet. We demonstrate this for the droplets frozen on the inclined surface of a wedge of low thermal diffusivity material while cooling the horizontal bottom surface of the wedge. The reported research on the droplet freezing mechanism and shape evolution may contribute to the understanding of aircraft and wind turbine icing, which is crucially important for engineering.

1.1. Materials

The following materials were used to manufacture the wedges:

1) Polymethylmethacrylate (abbreviated PMMA), CAS: 9011-14-7; supplied by Jumei Acrylic Manufacturing Co. Ltd. China.

2) Polytetrafluoroethylene (abbreviated PTFE), CAS: 9002-84-0; supplied by Wuxi Xiangjian PTFE Product Co. Ltd. China.
3) Polyurethane (abbreviated PU), CAS: 67700-43-0; supplied by Jiujiang Autai Rubber & Plastic Co. Ltd. China.
4) Titanium plates, supplied by Shaanxi Yunzhong Metal Technology Co. Ltd. China.

Physical properties of the substrates are summarized in Table 1. Bi-distilled water was used for the droplets. Bi-distilled water was obtained using a bi-distillator GFL-2102, GFL, Germany. Specific electric resistivity of water was $\rho = 17.8 \pm 0.5\,\mathrm{M\Omega} \times \mathrm{cm}$ as established at the temperature of t = 25 °C.

1.2. Methods

Small water droplets (V = 10±0.1 μl) were placed on the surface of the wedge using a precision micro-syringe. The geometric dimensions of the wedge, its location on the cooled metal plate and location of droplets are shown in Fig. 1.

The crystallization of water droplets was observed at two different points on the wedge surface, namely: at distances of 7.5 mm and 15 mm from the edge (see Fig. 1). As the distance from the sharp edge of the wedge increased, the droplet distance to the cooled surface also increased. The contact angles were measured using a laboratory goniometer (CRUSS DSA-100, GmbH) with the software CRUSS ADVANCE. Change in the droplet shape during its cooling and crystallization was monitored *in situ* with the digital video camera with a resolution of 1920 × 1200 pixel. Experiments were repeated five times; the results demonstrated satisfactory reproducibility.

1.3. Freezing of water droplets and temperature measurements

Cooling of the metal plate under the wedge was performed with the thermo-electric modulus with a power of W = 95 W enabling the maximal temperature change of 84 °C. The cooling rate was 20 ± 1 K/min. The surface temperature of the plate was controlled with the dual laser infrared sensor and the K-type thermocouple. Initial temperature and relative humidity (RH) in the experimental cell were set as T = 25 ± 0.5 °C and RH = 40 ± 1 %.

The testing was carried out with the experimental cell. The temperature control within the cooled working cell was carried out with three thermocouples: the first one measured the surface temperature of the cold plate, the second thermocouple measured the surface temperature of the wedge at the distance of 7.5 mm from the edge, and the third one – at the distance of 15 mm from the edge. Geometrical parameters of the cell are presented in Fig. 2.

Table 1
Physical properties of the substrates.

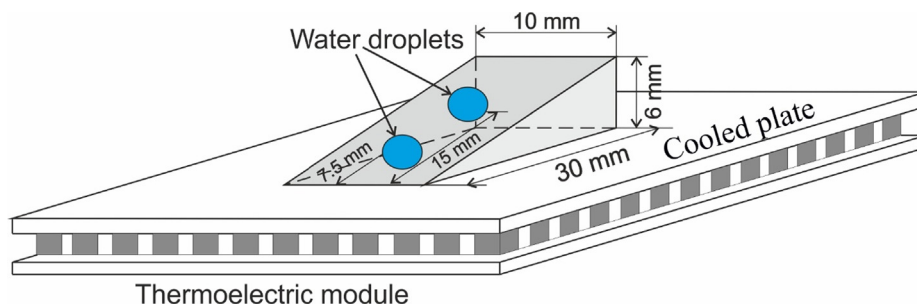| Material	Thermal diffusivity, κ, 10^{-6} m²/s	Apparent contact angle, $\theta°$
PMMA	0.11	70 ± 5
PTFE	0.11	85 ± 5
PU	0.09	75 ± 5
Ti	9.3	65 ± 5

Fig. 1. Arrangement of a polymer wedge and water droplets on the surface of a cooled plate is schematically shown.
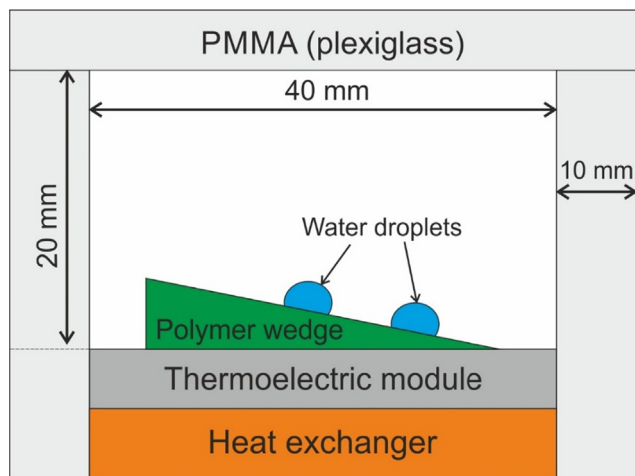

Fig. 2. Schematic representation of a thermally insulated cell is presented.

2. Experimental results

Water droplets were placed on the wedge made from various materials, as shown in Figs. 1,2 and frozen as described in Sections 1.2–1.3. Ice nucleation started from the solid/liquid interface as discussed in detail in refs. 24–25. The crystallization front propagated from the base (contact area) of the droplet towards its apex [24–25]. Typical freezing tip of the droplet, studied in refs. 7–14 was registered in all the experiments, as depicted in Fig. 3. Spatial orientation of the freezing tip (cone) was quantified by angle α formed by the normal to the surface and the axis of symmetry of the freezing tip, as shown in Fig. 4. The opening angle of the freezing tip was measured. The important methodological problem related to the experimental establishment of the opening angle should be pointed out and discussed. In principle, two different contact angles denoted ε_1 and ε_2, inherent for the presented experimental situation should be distinguished as shown in Fig. 3, namely: ε_1 is the opening angle formed by the freezing cone itself, whereas ε_2 is formed by the tangent to the droplet surface built from the apex of the droplet, as depicted in Fig. 3.

The aforementioned angles varied within the ranges $115 \pm 1^0 < \varepsilon_1 < 126 \pm 1^0$ and $125 \pm 1^0 < \varepsilon_2 < 140 \pm 1^0$ as shown in Fig. 3. The angle ε_2 arises from the distortion of the droplet itself and may be easily mixed with the "true" opening angle of the freezing cone ε_1, thus, giving rise to misinterpretation of the experimental results. The measured in our experiments opening angle of the freezing tip ε_1 was slightly lower than that reported in refs. 15–19. The possible reason for this is the aforementioned difficulty in experimental distinction between the angles ε_1 and ε_2. Both of angles ε_1 and ε_2 slightly decreased with the increase in the distance from the wedge bottom, as depicted in Fig. 3. One recognizes that

the drop situated further from the edge exhibited the opening angle of the freezing cone closer to the universally observed values in [15–19]. This observation can be presumably attributed to lower freezing time available for the drop close to the edge. The dependence is rather weak, and more or less compatible with observations in the aforementioned papers.

We conclude that the opening contact angle of the freezing cone ε_1 is confined within the narrow range for the substrates possessing very different thermal properties. Interfacial properties of the substrates quantified with the apparent contact angle θ are summarized in Table 1. Wettability of the studied surfaces was varied in a broad range, namely: $65 \pm 5^0 < \theta < 85 \pm 5^0$ (the large scattering of the contact angles is due to the contact angle hysteresis inevitable for droplets placed on the inclined surface [26–28]). Experimental findings evidence no influence of the apparent contact angle on the value of the opening angle of the freezing tip ε_1, thus, the supporting the idea of the universal mechanism of its formation, suggested in refs. 15–19. At the same time, the wetting properties of the wedge influenced the spatial orientation of the freezing tip, quantified by angle α (see Fig. 4) to be discussed below.

The acute angle of the wedge was equal $\beta = 11.3 + 0.1^\circ$ as depicted in Figs. 1–4. Two droplets were placed at different distances from the edge as shown in Figs. 1,2, and the resulting difference in the inclination angles of the freezing tips were recorded (see Fig. 4). The inclination angle α varied in a broad range of $0.8^\circ \pm 0.1 < \alpha < 19^\circ \pm 1$. In other words, the axis of the freezing tip does not coincide with the normal to the wedge surface. The physical meaning of this observation is discussed below.

We attribute the change in the tilt angle of the freezing cone to the change in the temperature gradient due to the low thermal conductivity of the wedge material. The change in the temperature gradient emerges from the growth in the thickness of the wedge taking place with increasing distance from the edge. Orientation of the ice cone at the final stage of crystallization allows one to assume the change in the direction of the temperature gradient. Obviously, the thermal diffusivity of the wedge material affects the local temperature gradients. The results obtained indicate that a decrease in the thermal diffusivity of the material (from Fig. 4A to Fig. 4B and 4C) leads to the corresponding increase in both the absolute value and direction of the temperature gradient. Note that the direction of the heat flux in an isotropic medium is opposite to the direction of the temperature gradient.

The wetting characteristics of the surface should be also taken into account. Although the thermal diffusivity of PTFE is almost the same as that of PMMA, the shift in the temperature gradient was less pronounced on PTFE, presumably due to the higher wetting angle (Fig. 4). Comparing the results with the droplet crystallization on the titanium surface, we can see that the temperature gradient on titanium substrates shifts in the direction normal to the surface (Fig. 5). Due to the high thermal diffusivity of titanium
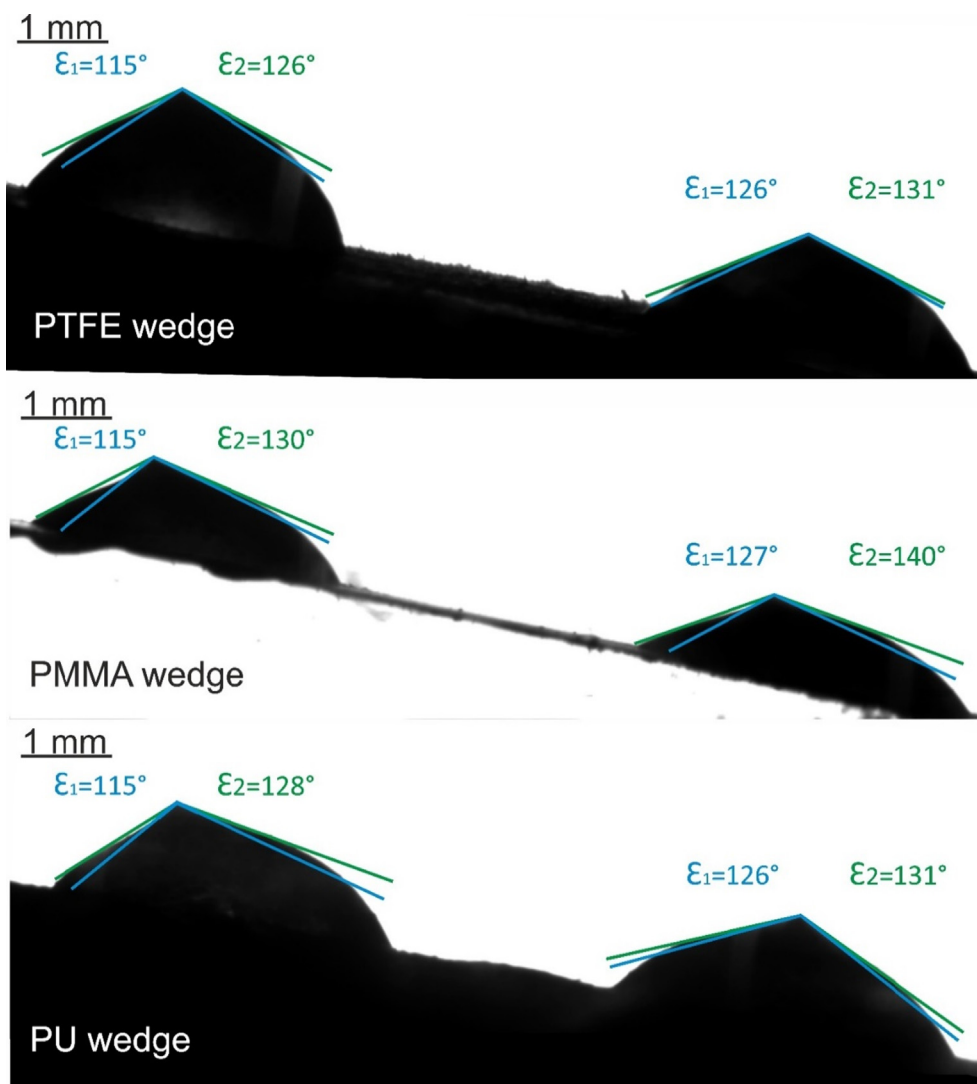
Fig. 3. Shapes and angles of the droplets frozen on different substrates are depicted. Angles ε_1 are ε_2 are depicted.

compared to polymers, the direction of the temperature gradient at the base of the droplet practically coincides with the direction of the normal to the wedge surface regardless of the droplet position (see Fig. 5).

3. Discussion

3.1. Qualitative analysis of the problem of water freezing

Let us start from the analysis of the dimensionless numbers relevant to the reported experimental situation. The Bond number, describing the interrelation between gravity and interfacial phenomena is supplied by Eq. (1):

$$\text{Bo} = \frac{\rho g R^2}{\gamma} \qquad (1)$$

where ρ and γ are the density and surface tension of water correspondingly and the R is the characteristic dimension of a droplet. Assuming $\rho = 10^3 \frac{\text{kg}}{\text{m}^3}; \gamma \cong 71 \times 10^{-3} \frac{\text{J}}{\text{m}^2}$ and $R \cong 2.5\text{mm}$ yields estimation Bo $\cong 1$. In other terms, the effects of gravity and interfacial tension are comparable.

$\Psi\Psi$

$$\Psi = \frac{E_{surf}}{E_{bulk}} \cong \frac{2\pi\gamma R^2}{c_p \rho \frac{2}{3}\pi R^3 \Delta T} = \frac{3\gamma}{c_p \rho R \Delta T} \qquad (2)$$

where $E_{surf} \cong 2\pi\gamma R^2$ is a rough estimation of the surface energy of a droplet seen a hemisphere, $E_{bulk} \cong c_p \frac{2}{3}\rho\pi R^3 \Delta T$ is the heat necessary for cooling the droplet, where $c_p \cong 4186 \frac{\text{J}}{\text{kg} \times \text{K}}$ is the specific heat capacity of water and $\Delta T \cong 20\text{K}$ is the temperature difference in the freezing droplet. Substituting of the aforementioned values of physical parameters in Eq. (2) yields the value of $\Psi \cong 2.0 \times 10^{-6}$; this means that the bulk effects due to freezing dominate the effects due to the gravity and surface tension.

3.2. Calculations of temperature field in the polymer wedge

The temperature measurements at two points on the cold plate surface confirmed that the plate under the wedge can be considered isothermal. The calculations did not take into account the effect of the finite width of the wedge and considered the temperature field in the symmetry plane of the wedge, where the temperature measurements were carried out. The influence of the droplets on the wedge temperature field is negligible even near the droplets and was not considered in the calculations.
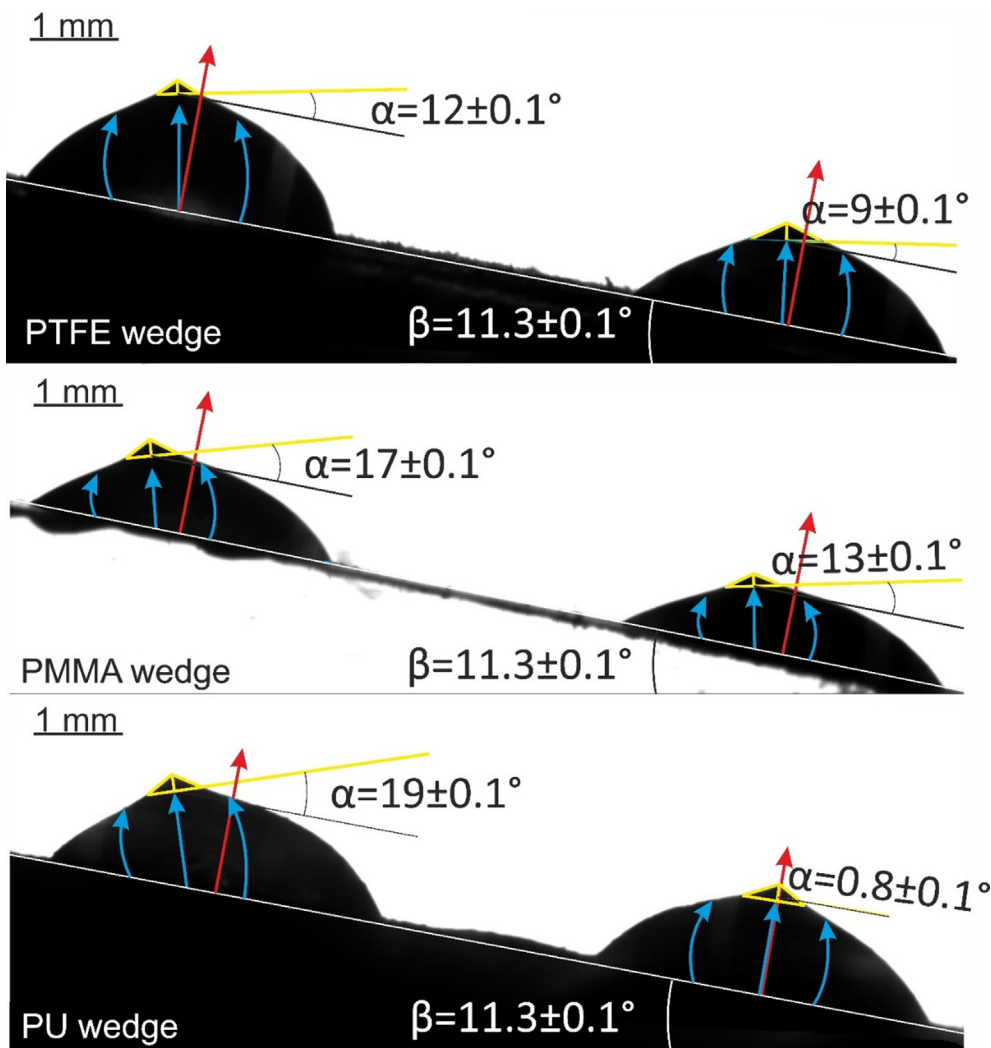
Fig. 4. Crystallization of water droplets on the surface of polymer wedges: (A) PTFE; (B) PMMA; (C) PU (red line is the normal to the wedge surface). α is the angle of inclination of the freezing tip axis relative to the normal to the surface; β is the wedge angle. Temperature gradient lines are qualitatively shown in blue. (For interpretation of the references to colour in this figure legend, the reader is referred to the web version of this article.)
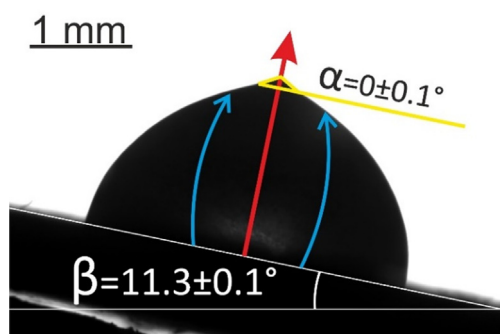

Fig. 5. Water droplet crystallization on the wedge made of titanium (red line depicts the normal to the inclined surface). (For interpretation of the references to colour in this figure legend, the reader is referred to the web version of this article.)

In this section, we will look at the most interesting case, when the wedge is made of dense polyurethane, which has the lowest thermal conductivity. The results of measurements of the temperature of the inclined wedge surface in the symmetry plane are shown in Fig. 6. It can be seen that the cooling lag between the central point of the wedge surface (T_2) and the cold plate temperature

(T_1) increases from the beginning of the process, reaching a maximum after about 30–40 s, and then decreases. The quasi-steady thermal regime with an almost linear temperature profile along
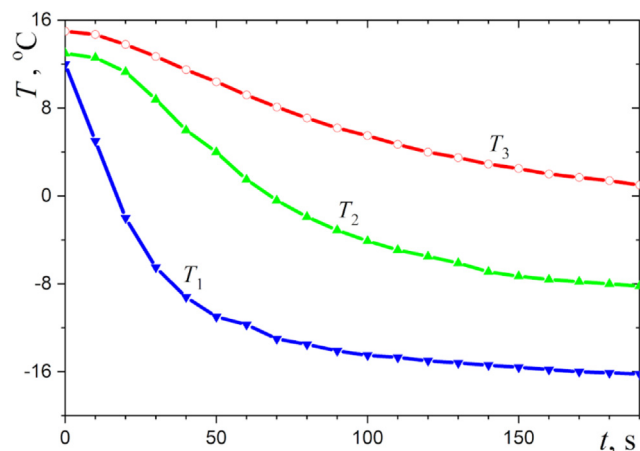

Fig. 6. Temperature of the inclined wedge surface: T_1 – at the top of the wedge, T_2 – in the middle of the surface, T_3 – at the maximum distance from the top of the wedge.

the inclined surface of the wedge occurs about two minutes after the start of cooling. Note that the temperature of the upper point of the wedge surface (T_3) is slightly above 0 °C even at t = 190 s. Therefore, experiments with freezing of water droplets can be performed only at some distance from the upper point. The following simple interpolation was used for the temperature of the inclined surface of the wedge:

$$T\left(t, \bar{s}\right) = T_1(t) + A(t)\,\bar{s} + B(t)\bar{s}^2, \ \bar{s} = s/s_{max}, \ 0 \le s \le s_{max} \quad (3a)$$

$$A(t) = 4T_2(t) - 3T_1(t) - T_3(t), \ B = 2(T_3(t) - 2T_2(t) + T_1(t)) \quad (3b)$$

where s is the distance from the top of the wedge, $s_{max} = \sqrt{L^2 + H^2}$, L is the length of the horizonal side of the wedge, H is the wedge height.

When calculating the temperature field, $T(t, x, y)$, in the symmetry plane of the polymer wedge, it was assumed that the thermophysical properties of the polymer are independent of the temperature. The following transient equation of heat conduction was solved:

$$\frac{1}{\kappa}\frac{\partial T}{\partial t} = \frac{\partial^2 T}{\partial x^2} + \frac{\partial^2 T}{\partial y^2} \quad (4)$$

where κ is the thermal diffusivity of the polymer, x is the horizontal coordinate measured from the top of the wedge, y is the vertical coordinate measured from the same point. On all surfaces of the wedge a boundary condition of the first kind can be set: on the horizontal surface – the known temperature of the metal plate, on the inclined surface – the interpolation of the measured temperatures (3a,b), on the vertical surface – the following linear interpolation:

$$T(t, L, y) = T_1(t) + (T_3(t) - T_1(t))\frac{y}{H} \quad (5)$$

The non-uniform initial temperature was set as follows:

$$T(0, x, y) = T_1(0) + (T_3(0) - T_1(0))\frac{xy}{LH} \quad (6)$$

The conduction problem was solved using a purely implicit finite-difference scheme of second order approximation on an orthogonal grid with splitting the differential operator in the right-hand side of Eq. (4) into two parts and alternating numerical solutions along the grid lines in the horizontal and vertical directions [29]. A computer program developed by one of the authors was used in the calculations. The peculiarity of the computational region at the top of the wedge was avoided by removing a small segment $x < x_{min} = L/20$ and setting a boundary condition of the first kind on the surface $x = x_{min}$. This boundary condition was formulated similarly to the condition on the vertical surface $x = L$. A rectangular grid with 200 intervals in the vertical direction and 190 intervals in the horizontal direction was used. The minimum time integration step was 0.01 s. Without focusing on the finite-difference approximation, we note that similar algorithms of numerical solution have been used in recent works [24,30,31].

Fig. 7 shows the calculated temperature fields at different moments of time. For cooling and solidification of two water droplets shown schematically in Fig. 7, the most interesting are the numerical data at t = 1 min, when the lower drop is already freezing and the upper drop has not yet started to freeze. At t = 30 s both droplets are only cooled to different degrees but not yet solidified, and at t = 2 min the upper droplet solidifies as well. It is interesting that at t = 1 min the directions of the heat flux below
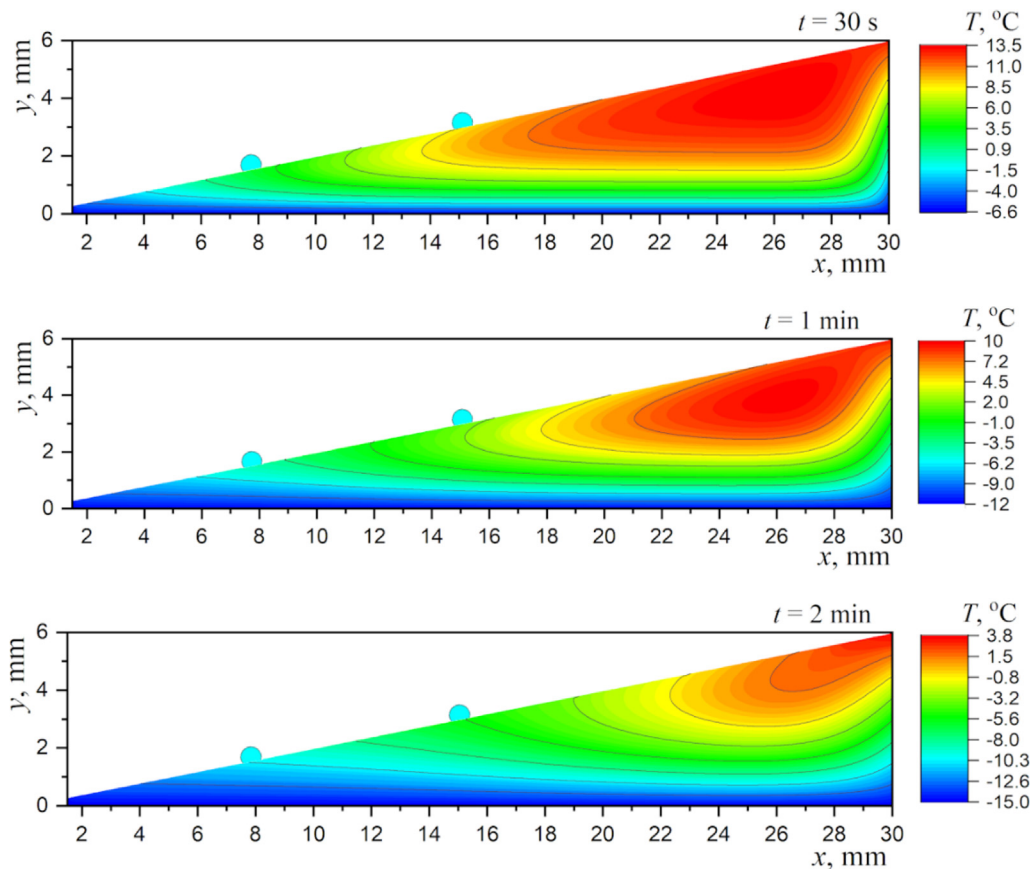

Fig. 7. Calculated temperature fields in the polymer wedge.

the lower and the upper droplets differ significantly, which explains the different orientation of the ice cones formed on the droplet surface at the completion of their crystallization.

Thus, we conclude that the axis of the freezing cone follows the direction of the temperature gradient imposed on the cooled droplet, which in turn governs, the direction of the crystallization front within the droplet [15–17].

4. Conclusions

Freezing of droplets, placed on the cooled surfaces gives rise to the effects, which are very different from those observed for "free frozen droplets" suspended in atmosphere [32]. One of these effects is the formation of the so-called freezing cone (or freezing tip), which was subjected to intensive experimental and theoretical research recently [15–19]. We investigated freezing of water droplets placed on the inclined surface of a wedge with a cooled lower horizontal bottom surface. The experiments with very different materials of the wedge (including polymers and metal) were conducted. In all cases, the shape of the droplets was continuously monitored during their freezing. The opening angle of the freezing tip turned out to be independent of the interfacial and thermal properties of the substrate material; thus, supporting the universal mechanism of formation of the freezing cone, introduced in refs. 15–19. Note that, this angle decreases slightly with the distance from the polymer wedge bottom.

We hypothesized that the orientation of the freezing tip is controlled by the direction of heat flux at the base of the sessile droplet. This was confirmed in a series of laboratory experiments. Various spatial orientations of the freezing tip of the droplets on the polymer wedge were obtained for the first time. This result was explained using the numerical modeling of the transient temperature field in the wedge. As one might expect, the freezing tip orientation is determined by the direction of heat flux (or temperature gradient) at the contact surface of the droplet, which in turn governs the orientation of the crystallization front within a cooled droplet. The axis of the freezing cone approaches to the wedge normal with the increase in the thermal diffusivity of the substrate. In particular, for the titanium wedge the freezing tip is on the normal to the wedge surface. On the contrary, for the polyurethane wedges the angles between the normal to the wedge surface and the axis of the cone as high as $19 \pm 0.1°$ were registered. We conclude, that the spatial orientation of the freezing cone is governed to a much extent by the direction of the temperature gradient on the contact surface of the sessile water droplet. It should also be emphasized that the wetting properties of the wedge material, quantified by the apparent contact angle and contact angle hysteresis [26–28], influence the spatial orientation of the freezing tip. Thus, we demonstrate that the contact angle hysteresis impacts not only the time delay of icing, as shown in ref. 11, but also influences the formation of the freezing tip. In our future investigations we plan to study formation of the freezing shapes of droplets containing water-soluble polymers and colloidal systems.

CRediT authorship contribution statement

Anton Starostin: Investigation, Methodology, Visualization, Writing – original draft. **Vladimir Strelnikov:** Data curation, Supervision, Writing – original draft. **Leonid A. Dombrovsky:** Investigation, Methodology, Software, Writing – review & editing. **Shraga Shoval:** Investigation, Methodology, Writing – review & editing. **Oleg Gendelman:** Conceptualization, Investigation, Methodology, Writing – original draft, Methodology, Writing –

review & editing. **Edward Bormashenko:** Conceptualization, Investigation, Methodology, Supervision, Writing – original draft, Methodology, Writing – review & editing.

Declaration of Competing Interest

The authors declare that they have no known competing financial interests or personal relationships that could have appeared to influence the work reported in this paper.

Acknowledgements

References

[1] F. Chu, S. Gao, X. Zhang, X. Wu, D. Wen, Droplet re-icing characteristics on a superhydrophobic surface, Appl. Phys. Lett. 115 (2019) 073703.

[2] T. Zhang, L. Wang, Z.h. Wang, J. Li, J. Wang, Single ice crystal growth with controlled orientation during directional freezing, J. Phys. Chem. B 125 (3) (2021) 970–979.

[3] A.-M. Kietzig, S.G. Hatzikiriakosa, P. Englezos, Physics of ice friction, J. Appl. Phys. 107 (2010) 081101.

[4] E.J.Y. Ling, V. Uong, J.-S. Renault-Crispo, A.-M. Kietzig, P.h. Servio, Reducing ice adhesion on nonsmooth metallic surfaces: wettability and topography effects, ACS Appl. Mater. Interfaces 8 (13) (2016) 8789–8800.

[5] E. Fagerström, A.-L. Ljung, L. Karlsson, H. Lycksam, Influence of substrate material on flow in freezing water droplets – an experimental study, Water 13 (12) (2021) 1628.

[6] S. Xue, Y. Liu, Y. Wang, B. Xiao, X. Shi, J. Yao, X. Lv, W. Yuan, Y. He, Variation in anti-icing power of superhydrophobic electrothermal film under different temperatures and wind speeds, Int. J. Aerospace Eng. 2022 (2022) 3465428.

[7] X. Shi, X. Lv, J. Lu, Y. Xu, W. Yuan, Y. He, Anti-icing polyimide thin film with microcolumns fabricated by RIE with cooling and PCVD, Micro Nano Lett. 17 (1) (2022) 1–8.

[8] A. Starostin, V. Strelnikov, V. Valtsifer, I. Lebedeva, I. Legchenkova, E. Bormashenko, Robust icephobic coating based on the spiky fluorinated Al_2O_3 particles, Sci. Rep. 11 (2021) 5394.

[9] I.V. Roisman, C. Tropea, Wetting and icing of surfaces, Curr. Opinion Colloid Interface Sci. 53 (2021) 101400.

[10] J.E. Castillo, Y. Huang, Z. Pan, J.A. Weibel, Quantifying the pathways of latent heat dissipation during droplet freezing on cooled substrates, Int. J. Heat Mass Transfer 164 (2021) 120608.

[11] M.A. Sarshar, C. Swarctz, S. Hunter, J. Simpson, Ch-H. Choi, Effects of contact angle hysteresis on ice adhesion and growth on superhydrophobic surfaces under dynamic flow conditions, Colloid Polym. Sci. 291 (2013) 427–435.

[12] W.-Z. Fang, F. Zhua, W.-Q. Tao, C. Yang, How different freezing morphologies of impacting droplets form, J. Colloid Interface Sci. 584 (2021) 403–410.

[13] Y. Li, M. Li, C. Dang, X. Liu, Effects of dissolved gas on the nucleation and growth of ice crystals in freezing droplets, Int. J. Heat Mass Transfer 184 (2022) 122334.

[14] T. Tao, X.F. Peng, D.J. Lee, Force of a gas bubble on a foreign particle in front of a freezing interface, J. Colloid Interface Sci. 280 (2004) 409–416.

[15] J.H. Snoeijer, P. Brunet, Pointy ice-drops: How water freezes into a singular shape, Am. J. Phys. 80 (9) (2012) 764–771.

[16] A.G. Marin, O.R. Enríquez, P. Brunet, P. Colinet, J.H. Snoeijer, Universality of tip singularity formation in freezing water drops, Phys. Rev. Lett. 113 (5) (2014) 054301.

[17] A. Schetnikov, V. Matiunin, V. Chernov, Conical shape of frozen water droplets, Am. J. Phys. 83 (1) (2015) 36–38.

[18] X. Zhang, X. Liu, J. Min, X. Wu, Shape variation and unique tip formation of a sessile water droplet during freezing, Appl. Therm. Eng. 147 (2019) 927–934.

[19] M.F. Ismail, P.R. Waghmare, Universality in freezing of an asymmetric drop, Appl. Phys. Lett. 109 (23) (2016) 234105.

[20] F. Boulogne, A. Salonen, Drop freezing: Fine detection of contaminants by measuring the tip angle, Appl. Phys. Lett. 116 (2020) 103701.

[21] Y. Zhao, C. Yang, P. Cheng, Freezing of a nanofluid droplet: From a pointy tip to flat plateau, Appl. Phys. Lett. 118 (201) (2021) 141602.

[22] X. Li, J. Yu, D. Hu, Q. Li, X. Chen, Freezing of nanofluid droplets on superhydrophobic surfaces, Langmuir 36 (43) (2020) 13034–13040.

[23] D. Zang, K. Lin, W. Wang, Y. Gu, Y. Zhang, X. Geng, B.P. Binks, Tunable shape transformation of freezing liquid water marbles, Soft Matter 10 (9) (2014) 1309–1314.

[24] A. Starostin, V. Strelnikov, L.A. Dombrovsky, S. Shoval, E. Bormashenko, Three scenarios of freezing of liquid marbles, Coll. Surf. A 636 (2021) 128125.

[25] A. Starostin, V. Strelnikov, L. A. Dombrovsky, S. Shoval, Ed. Bormashenko, On the universality of shapes of the freezing water droplets, Colloid & Interface Sci. Comm. 47 (2022) 100590.

[26] R. Tadmor, Open problems in wetting phenomena: Pinning retention forces, Langmuir 37 (21) (2021) 6357–6372.

[27] R. Tadmor, P.S. Yadav, As-placed contact angles for sessile drops, J. Colloid Interface Sci. 317 (2008) 241–246.

[28] R. Tadmor, Approaches in wetting phenomena, Soft Matter 7 (5) (2011) 1577–1580.

[29] M. Shashkov, Conservative Finite-Difference Methods on General Grids, CRC Press, New York (2018).

[30] A.A. Fedorets, L.A. Dombrovsky, Generation of levitating droplet clusters above the locally heated water surface: A thermal analysis of modified installation, Int. J. Heat Mass Transfer 104 (2017) 1268–1274.

[31] M. Frenkel, L.A. Dombrovsky, V. Multanen, V. Danchuk, I. Legchenkova, S. Shoval, Y. Bormashenko, B.P. Binks, E. Bormashenko, Self-propulsion of water-supported liquid marbles filled with sulfuric acid, J. Phys. Chem. B 122 (32) (2018) 7936–7942.

[32] J. Kleinheins, A. Kiselev, A. Keinert, M. Kind, T. Leisner, Thermal imaging of freezing drizzle droplets: pressure release events as a source of secondary ice particles, J. Atmosph. Sci. 78 (5) (2021) 1703–1713.